Effective Generation of Molecular Cavities in Polarizable Continuum Model by DefPol Procedure

CHRISTIAN SILVIO POMELLI,[1] JACOPO TOMASI,[1] MAURIZIO COSSI,[2] VINCENZO BARONE[2]

[1]*Dipartimento di Chimica e Chimica Industriale, Universitá degli Studi di Pisa, via Risorgimento 35, I-56100 Pisa, Italy*

[2]*Dipartimento di Chimica, Universitá Federico II, via Mezzocannone 4, I-80134 Napoli, Italy*

Received 25 May 1999; accepted 16 July 1999

ABSTRACT: A new computational strategy for the building of molecular cavities (named DefPol) has been linked to the most recent implementation of the polarizable continuum model (PCM) for the representation of solvent effects on physicochemical properties of large molecules. Free energies, analytical gradients, and Hessians can be computed in this framework in the rigid cavity approximation. Coupling DefPol cavities with a number of other recent improvements of the standard algorithm (e.g., effective use of symmetry, iterative procedures with linear scaling) significantly enlarges the dimensions of systems amenable to refined computations and strongly reduces the gap between computations for isolated molecules and in solution. © 1999 John Wiley & Sons, Inc. J Comput Chem 20: 1693–1701, 1999

Keywords: solvation; molecular surface; polarizable continuum model

Introduction

Recent progress in hardware and software is pushing the dimensions of systems amenable to reliable quantum mechanical (QM) investigations toward biomolecules and materials of technological significance.[1, 2] However, many physicochemical processes involving those systems take place in liquid solutions, and often an accurate theoretical treatment of such processes cannot leave a realistic description of the environmental effects aside. As a consequence, there is an urgent need of fundamental and algorithmic developments approaching the target that all the computational models developed for systems *in vacuo* can also be used (with comparable resources) in solution. Among the several strategies proposed so far, continuum models are becoming more and more popular because of their flexibility and efficiency.[3–6] Here we are concerned in particular with the polarizable continuum

Correspondence to: C. S. Pomelli or M. Cossi; e-mails: cris@balder.dcci.unipi.it or cossi@marcos.dichi.unina.it

Contract/grant sponsor: C.N.R. through Progetto Strategico Computational Modeling of Complex Molecular Systems

CCC 0192-8651 / 99 / 161693-09

model (PCM),[3,7,8] which, thanks to recent developments in the underlying model and in the numerical implementation,[8–16] gives structural and energetic data approaching the so-called chemical accuracy. Furthermore, we are rapidly reaching the situation in which all the QM procedures (including analytical gradients and second derivatives) available for molecules *in vacuo* are also available (with comparable computational efficiency) for systems in solution.[11–14,16] Because the PCM was developed in the last years with special reference to sophisticated QM models, its most effective use for very large systems requires some modifications concerning the evaluation of polarization charges[15,17] and the building of the molecular cavity.[18,19]

In this framework this article is devoted to the improvement and validation of a recent algorithm (DefPol)[19] for the generation of molecular cavities (to replace the standard Gepol algorithm[20]) with a very favorable scaling with the dimensions of the solute. This new implementation allows the computation of free energies and of analytical first and second derivatives in the rigid cavity approximation, making use of recent linear scaling techniques[16] and of symmetry.[15] With the expression "rigid cavity approximation" we mean that the procedure neglects some contributions to the free energy derivatives due to the cavity [see eq. (15)] and not of maintaining a fixed cavity during the geometry optimization. This approximation was introduced and tested in preceding studies (see ref. 14 and references therein): the numerical deviations of each single derivative with respect to a complete calculation are quite limited, and its effect on the final geometry optimization is almost irrelevant. The whole procedure was implemented in the development version of the Gaussian series of programs,[21] thus allowing the use of several QM, molecular mechanical (MM), and QM/MM (ONIOM[22]) methods.

DefPol ALGORITHM

As in other continuum solvation methods, in PCM the solute molecule is embedded in a cavity surrounded by a polarizable medium with the dielectric constant of the solvent. Cavities modeled on the solute shape can be obtained starting from a shape function[19] expressed as the union of hard sphere shape functions $f_{hs}(A)$ centered on N atoms and/or atomic groups of the molecule M:

$$f_{hs}(M) = \bigvee_G f_{hs}(G) \quad G \in M, \tag{1}$$

where $\bigvee$ is the logical operator "or", which runs on all the groups and hence on the spheres, and

$$f_{hs}(G) = f_{hs}(\mathbf{r}; \lambda(G), R_{eff}(G), \mathbf{R}_G) \tag{2}$$

is the shape function related to the effective radius of group G, $R_{eff}(G)$, modified by a suitable numerical factor λ, and depending on the $\mathbf{R}_G$ position of the group.

The use of the shape function concept greatly simplifies cavity definition. With definition (1) in particular we immediately arrive at the molecular cavity characterized by the volume V_M and the surface S_M, which is adequate for the computation of cavitation energies (*vide infra*) but not for other components of the solvation energy. In particular, other nonelectrostatic contributions are better represented in terms of the so-called solvent accessible surface S_{SA}, which is defined as the close surface described by the center of a sphere with radius R_S representing the solvent in its movement around the solute. This merely corresponds to an increment of R_S to all the hard sphere shape functions. To describe electrostatic contributions to solvation energies it is convenient to resort to the solvent excluding surface S_{SE} that is defined as the surface limiting the portion of space not accessible to the solvent molecules. The corresponding cavity may be defined in terms of f_{hs} supplemented by an obstruction function, such that

$$f_{SE}(M) = f_{hs} \vee f_{obs}. \tag{3}$$

Because the DefPol procedure is already described in detail in an article published in a recent volume of this journal,[19] here we give only a short overview of its characteristics, pointing out the improvements added in the Gaussian implementation.

The DefPol procedure builds a molecular surface by applying successive deformations to a polyhedron inscribed in a sphere. The first two steps are the building of the polyhedron, which is performed by the PolyGen algorithm[18] already implemented in Gaussian[17,18] and its projection on the inertia ellipsoid of the molecule magnified by a factor τ. In order to avoid isotopic dependent cavities, atomic numbers are used in place of atomic masses in this step and any initial vertex is projected onto the ellipsoid according to

$$\mathbf{v} \rightarrow \tau[b_1(\mathbf{v}_1 \cdot \mathbf{x}_1)\mathbf{x}_1 + b_2(\mathbf{v}_2 \cdot \mathbf{x}_2)\mathbf{x}_2 + b_3(\mathbf{v}_3 \cdot \mathbf{x}_3)\mathbf{x}_3], \tag{4}$$

where b_1, b_2, and b_3 are the half-axes of the ellipsoid.

Next the vertices and the centers of the tesserae are displaced on the appropriate surface. The original formulation of DefPol employs a numerical algorithm to find the boundary (i.e., the surface) of the shape function and hence the tesserae edges.

The new version instead employs an essentially analytical method in which just a few numerical steps still survive. In particular, the vertices are moved on straight lines from their original positions to the cavity surface,

$$\mathbf{v} = \mathbf{v}_0 + \delta \mathbf{v}_1, \tag{5}$$

where $\mathbf{v}_0$ is the original position of the vertex and

$$\mathbf{v}_1 = -\mathbf{v}_0/|\mathbf{v}_0|. \tag{6}$$

Thus, for $0 < \delta < 1$ all the points lie between the starting vertex and the center of the ellipsoid (here taken as the axis origin).

In this article we introduce a fully analytical determination of the vertex positions considering the geometrical nature of the shape function components: spheres and tori. One has to evaluate all the intersections among the straight line defined in (5) and all the geometric components of the shape function or, even better, the reduced number determined by the procedure described in the following. The line–sphere intersection problem leads to a second-degree equation

$$\delta^2 + 2\delta(\mathbf{v}_0 - \mathbf{r}) \cdot \mathbf{v}_1 + |\mathbf{v}_0 - \mathbf{r}|^2 - R^2 = 0, \tag{7}$$

where $\mathbf{r}$ and R are the center and the radius of the sphere, respectively. The correct solution is always the smallest satisfying eq. (7).

The line–torus intersection problem instead leads to a fourth-degree equation. We do not report this equation because we did not find a sufficiently robust general solution among the several available methods.[23] Thus, we resort to a two-stage procedure in which a first analytical guess corresponding to the position of the vertex on the sphere circumscribing the two-atom term is refined by the same numerical procedure used in the original implementation,[19] which is however now much more rapidly convergent because of the effective initial guess.

As mentioned above, the procedure for the evaluation of the shape function is also now considerably enhanced. There are three types of terms in the DefPol shape function:

(1) Atomic terms consisting of a simple sphere. In this case the position of a vertex is determined analytically [eq. (7)].
(2) Two-atom terms consisting of a torus supplemented by a sphere that circumscribes the volume occupied by the shape function term. The position of the vertex is determined by the composite procedure described above.

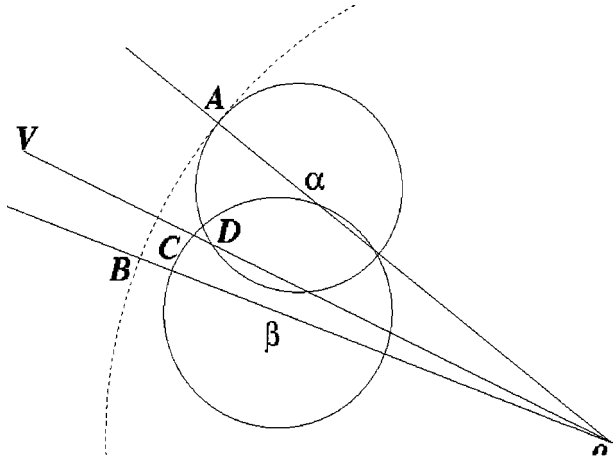

FIGURE 1. In the strategy for the evaluation of the shape function the sphere α is taken into consideration before the sphere β, but the right final position of vertex *V* is *C* not *D* because the segment *VC* is shorter than the segment *VD*.

(3) Three-atom terms consisting of a couple of spheres supplemented by a further sphere analogous to that defined for the two-atom terms. In this case we have to solve two second-degree equations and to choose among the four solutions the smallest one lying inside the circumscribed sphere.

The problem is now to find in the most efficient way the nature of the shape function term on which the vertex will reside, examining in this scope the smallest possible number of candidates. The "good" intersection corresponds to the point closest to the original vertex position, thus to the smallest value of δ. Then we define for each shape function term

$$\mu_i = |\mathbf{r}_i| + R_i, \tag{8}$$

where $\mathbf{r}_i$ is the position of the atom for the single-atom terms and the center of the circumscribed sphere in the other cases and R_i is the radius of the sphere centered on $\mathbf{r}_i$. Thus, μ_i represents the point of the ith term in the shape function most distant from the origin.

The candidate shape function terms are analyzed in the order of decreasing μ by simply assigning an index to each term and sorting the indexes with respect to μ values. The procedure is not terminated when the first intersection is found because other terms can lead to intersections with lower δ values (an example is shown in Fig. 1).

Thus, one has $\delta_f \geq \delta_g$ where δ_f corresponds to the first intersection and δ_g to the good one. Furthermore, for each intersection the following inequality

holds:

$$\delta \geq |\mathbf{v}_0| - \mu. \tag{9}$$

Rearrangement of this equation and application to the good intersection leads to

$$\mu_g \geq |\mathbf{v}_0| - \delta_g \geq |\mathbf{v}_0| - \delta_f. \tag{10}$$

The remaining shape function terms must be evaluated only until the value in the last term of inequality (10) is reached, thus drastically reducing the number of computations.

This strategy cannot be applied to tesserae centers using the positions and search directions defined in the original version of DefPol.[19] Thus, the initial center position for each tessera is now defined as the average of the corresponding vertex positions and the same can be done for its displacement toward the center of the cavity. Several tests showed that this new definition does not lead to formal or numerical problems when integrated in the full DefPol algorithm.

The further steps of the procedure are not changed with respect to the original version. The volume of the tetrahedron defined by its vertices and its undisplaced center has to be computed for each triangle j, and if this volume is larger than a previous defined threshold (usually 0.5 Å^3) we proceed to triangle division. This recursive generation ends up with a deformed polyhedron with metric and topology different from the original one. As a final step this polyhedron composed of flat triangles is transformed into a polyhedron composed of spherical triangles.[19] This completes the description of the algorithm implemented in the Gaussian package.

SOLVATION FREE ENERGY AND ITS DERIVATIVES

The size of the atomic and group spheres used to define the shape function is a delicate parameter in the calculation of solvation free energy; here we adopt our recent united atom topological model (UATM) in which the basic radius of non-hydrogen atoms is corrected by some topological indexes (hybridization, formal charge, nature of nearest neighbors), whereas hydrogens do not generate individual spheres but rather increase the radius of the spheres connected to atoms to which they are bonded.[8] In the same model the initial parameter λ of 1.4 is reduced by 0.1 if the solvent has H-bonding donor or acceptor abilities. Thus, the usual value $\lambda = 1.2$ is recovered for water whereas nonpolar solvents have λ values closer to those recently optimized by Luque et al.[24] We recall that the whole procedure is fully automated in the Gaussian package and leads to average errors of 0.2 and 1.0 kcal/mol for the solvation free energies of a large set of neutral and charged solutes, respectively.[8]

The solvation free energy can be partitioned into the following terms:

$$G = G_{el} + G_{cav} + G_{dis} + G_{rep}. \tag{11}$$

The free energy associated with the formation of the cavity in the solvent, G_{cav}, is calculated with the expression derived by Pierotti from the hard spheres theory[25] adapted to the case of nonspherical cavities.[26] The dispersion and repulsion terms (G_{dis}, G_{rep}) are calculated following Floris et al.'s procedure[27] with the parameters proposed by Caillet and Claverie.[28] All these terms are the same in QM and MM implementations. On the other hand, the electrostatic contribution can be written as

$$G_{el} = \frac{1}{2}\int_S \sigma(\mathbf{r})V(\mathbf{r})\,dS, \tag{12}$$

where σ is the induced surface charge density and $V(\mathbf{r})$ is the electrostatic potential created by the solute at point $\mathbf{r}$ of the cavity surface. Using the DefPol tessellation of the surface, eq. (12) can be approximated as

$$G_{el} = \frac{1}{2}\sum_i^{\text{tesserae}} q_i V(\mathbf{r}_i), \tag{13}$$

with $q_i = \sigma_i a_i$, σ_i being the charge density of tessera i.

Different algorithms corresponding to different mathematical approaches were proposed to determine the solvation charges q_i.[7, 8, 11, 13] They have the general expression

$$\mathbf{Dq} = -\mathbf{b}, \tag{14}$$

where the column matrix $\mathbf{q}$ collects the solvation charges and $\mathbf{D}$ is a square matrix of dimensions equal to the number of tesserae depending on the dielectric constant of the solvent (ϵ) and on tesserae geometrical parameters (actual definitions depend on the mathematical approach). The $\mathbf{b}$ column matrix collects the values of an electrostatic solute's quantity (the potential or the normal component of the electric field, depending on the approach selected). The $\mathbf{b}$ elements can be obtained in QM methods via the solution of the pertinent effective Schrödinger equation and in MM procedures from suitable atomic charges (and possibly polarizabilities).

A very effective algorithm for the computation of the derivative of G_{el} was given recently that can be applied to all the variants of PCM.[11–13] It leads to the addition of the following term to the gradient of

TABLE I.
DefPol/Gepol Comparison with the UFF Method[30] for 20 Small Molecules.

	DPCM			CPCM		
Molecule	Gepol	DefPol	δ	Gepol	DefPol	δ
Acetic acid	−5.92	−6.01	0.09	−5.98	−6.09	0.11
Butylnitrile	−2.64	−2.63	0.01	−2.65	−2.65	0.00
Chloromethane	−5.99	−5.98	0.01	−6.02	−6.02	0.00
Diethylsulfide	*−4.00*	*−4.21*	*0.21*	*−4.03*	*−4.06*	*0.03*
Difluoroethane	−13.23	−13.33	0.10	−13.40	−13.44	0.04
Dimethylamine	−2.94	−3.02	0.08	−2.98	−3.04	0.06
Dimethylether	*−5.32*	*−5.48*	*0.16*	*−5.43*	*−5.48*	*0.05*
Ethane	−0.19	−0.20	0.01	−0.19	−0.20	0.01
Ethanol	−6.02	−6.11	0.09	−6.08	−6.16	0.08
Phenol	−5.53	−5.51	0.02	−5.60	−5.60	0.00
Phosphine	−0.18	−0.18	0.00	−0.18	−0.18	0.00
Water	−4.62	−4.60	0.02	−4.61	−4.64	0.03
Cyanidric acid	−1.47	−1.48	0.01	−1.48	−1.49	0.01
Methane	−0.08	−0.08	0.00	−0.08	−0.08	0.00
Methanol	−5.97	−6.00	0.03	−6.02	−6.05	0.03
Methylacetate	−5.93	−5.97	0.04	−5.99	−6.01	0.02
Methylamine	−2.74	−2.79	0.05	−2.75	−2.81	0.06
p-Dibromobenzene	*−9.06*	*−9.23*	*0.17*	*−9.15*	*−9.19*	*0.04*
Pyridine	−2.58	−2.65	0.07	−2.64	−2.66	0.02
Trichloroerthylene	−6.12	−6.02	0.10	−6.27	−6.31	0.04
Mean unsigned deviation			0.06			0.03

Electronic Solvation free energies are in kilocalories per mole.

the isolated molecule (determined, of course, with the electron density computed in solution):

$$\left[\frac{1}{2}\sum_{i}^{\text{tesserae}} q_i V_i\right]^x = \sum_{i}^{\text{tesserae}} q_i V_i^x + \frac{2\pi\epsilon}{\epsilon - 1}\sum_{i\in\Gamma}\frac{q_i^2}{a_i}U_i(x), \quad (15)$$

where V_i^x is the partial derivative of V_i with respect to the parameter x and the last sum runs over the part of the cavity moving as a consequence of the nuclear displacement. The term $U_i(x)$ is related to tesserae geometrical parameters, which are not yet available in the DefPol model[19] (work is in progress). However, a number of studies[14] showed that the so-called rigid cavity approximation [in which the last term of eq. (15) is neglected] is often a good approximation for polar solutes in polar solvents. Under the same conditions the derivatives of nonelectrostatic contributions can also be neglected.

In the fixed cavity approximation the derivation of eq. (15) with respect to a second nuclear displacement, y, gives[14]

$$\left[\frac{1}{2}\sum_{i}^{\text{tesserae}} (q_i V_i)^x\right]^y = \sum_{i}^{\text{tesserae}} q_i V_i^{x,y} - \sum_{i}^{\text{tesserae}} D_{ij}^{-1} V_i^x V_j^y. \quad (16)$$

All the other terms entering QM computations of these derivatives remain unaltered from previous versions, so that we can also compare vibrational frequencies obtained with the new algorithm.

Results and Discussion

All the computations were performed with the development version of the Gaussian package[21] using the PBE0/6-31G(d)[29,30] methods for QM computations and the UFF force field[31] for MM computations. All the different versions of PCM were used for the evaluation of solvation free energies whereas, in view of the close similarity between the results of the different versions, only the conductor variant (C-PCM) was used for analytical

TABLE II.
Geometrical Parameters, Harmonic Vibrational Frequencies, Electrostatic Solvation Free Energies, and Dipole Moment Computed for H_2CO *In Vacuo* and in Water with DefPol and Gepol Cavities at PBE0/6-31G(d) Level.

	Vacuum	DefPol	Gepol
Geometrical parameter (Å, ∘)			
CH	1.110	1.108	1.108
CO	1.203	1.208	1.208
HCO	122.3	122.1	122.1
Harmonic frequencies (cm^{-1})			
$\nu_1(A')$	2495.9	2962.2	2960.9
$\nu_2(A')$	1882.0	1852.8	1851.7
$\nu_3(A')$	1565.1	1557.8	1557.6
$\nu_4(A')$	1204.2	1215.0	1215.0
$\nu_5(A'')$	3002.0	3031.8	3030.5
$\nu_6(A'')$	1282.8	1277.8	1277.6
Dipole moment (D)	2.220	2.673	2.672
Solvation free energy (Kcal/mol)		−2.72	−2.73

TABLE III.
Geometrical Parameters, Harmonic Vibrational Frequencies, Electrostatic Solvation Free Energies, and Dipole Moment Computed for H_2NO *In Vacuo* and in Water with DefPol and Gepol Cavities at PBE0/6-31G(d) Level.

	Vacuum	DefPol	Gepol
Geometrical parameter (Å, ∘)			
NH	1.019	1.026	1.026
NO	1.272	1.276	1.276
HNO	116.78	117.9	117.89
t	24.6	19.8	19.9
Harmonic frequencies (cm^{-1})			
$\nu_1(A')$	3431.4	3322.2	3321.4
$\nu_2(A')$	1706.7	1673.1	1674.7
$\nu_3(A')$	1443.8	1441.2	1441.1
$\nu_4(A')$	511.8	439.0	448.1
$\nu_5(A'')$	3552.1	3461.4	3460.4
$\nu_6(A'')$	1310.5	1283.2	1284.1
Dipole moment (D)	3.014	3.802	3.800
Solvation free energy (Kcal/mol)		−8.76	−8.74

derivatives. We employed the matrix inversion algorithm used in standard PCM codes, although more recent iterative implementations are more efficient for the evaluation of energies and gradients of large solutes.[15] Finally, all the computations may employ the symmetrization procedure recently implemented in the Gaussian package, which allows Abelian and non-Abelian symmetries in PCM computations of energies and their derivatives.[16]

The electrostatic component of the free energy of solvation evaluated at the UFF level are reported in Table I for Gepol and DefPol cavities with the original dielectric PCM (D-PCM) and the more recent C-PCM, thus leading to four series of data. The four series of numbers are very similar and the differences with respect to the changing of cavity type or electrostatic model are of the same order of magnitude. The unsigned error for each couple

of Gepol/DefPol data is reported. There are three cases (in italic in the Table) in which the discrepancies between Gepol and DefPol are very different in the D-PCM and C-PCM case. This can be ascribed to a larger sensitivity of D-PCM to local cavity irregularities. It is worthwhile to recall the analysis done by Klamt and Jones[32] about the low sensitivity of COSMO with respect to dielectric continuum formulations, which also apply to C-PCM. In two cases out of three the Gepol/D-PCM result is the one with a larger deviation with respect to the other three series of data, only in the diethylsulfide system the larger deviation is exhibited by the DefPol/D-PCM results.

Tables II and III contain the results obtained for two representative closed-shell (H_2CO) and open-shell (H_2NO) systems at the PBE0/6-31G(d) level. Once again Gepol and DefPol cavities lead to very close results for solvation free energies and the agreement is even better for energy derivatives. These results make us confident about the reliability and robustness of the new procedure for standard situations. However, the main reason behind the development of the DefPol model is its efficiency for large solutes. Although this was already analyzed in a previous article, here we illustrate a graphical comparison between the cavities, which was obtained for a finite-size nanotube, with Gepol and DefPol procedures (see Fig. 2).

The $C_{24k}B_{12k}N_{12k}H_{12}$ systems (the figure reports the system with $k = 1$) have a regular cylindrical structure[33] with a cylinder radius of $R = 4.96$ Å, which is not noticeably affected by solvent effects, and two sets of six H atoms at the ends of the tube. The obstruction function is more irregular at the end of the tube, and in these regions the higher smoothness of the DefPol procedure with respect to Gepol is evident. The solvation energies with D-PCM at the UFF level are -4.96 kcal/mol for Gepol and -4.91 kcal/mol for DefPol. The number of tesserae in these examples is 1500 for DefPol and 2099 for GEPOL; the gain in the CPU time for the part of the calculation related to the generation of the cavity is on the order of 1.8 for this case and it increases to $\sim$20 for the tube with $k = 20$ (containing 972 atoms).

Conclusion

The revised DefPol procedure we presented here presents some advantages with respect to the preceding one. One advantage is related to the analytical formulation of some intermediate steps in the definition of the shape function; this means a reduction in computational time and a higher stability

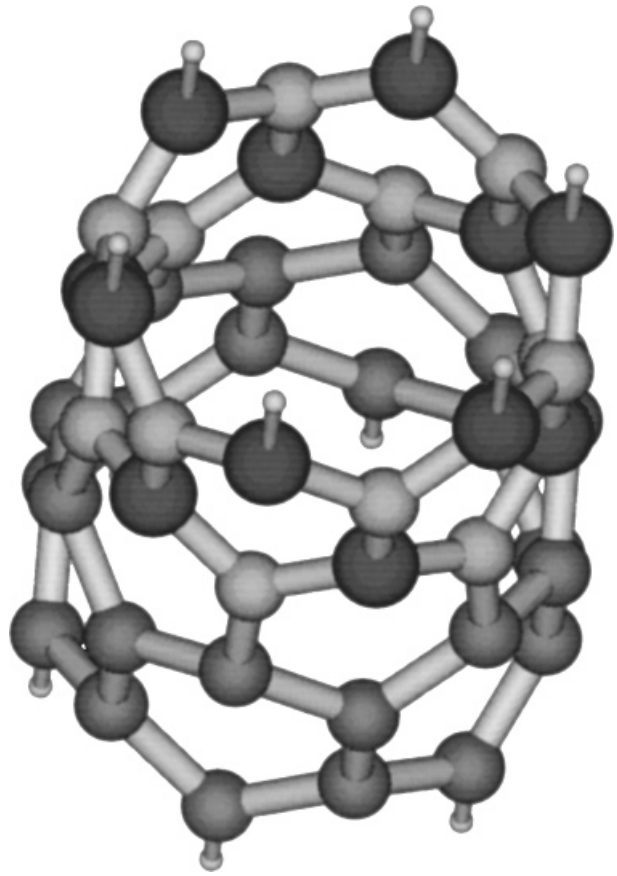

(a)

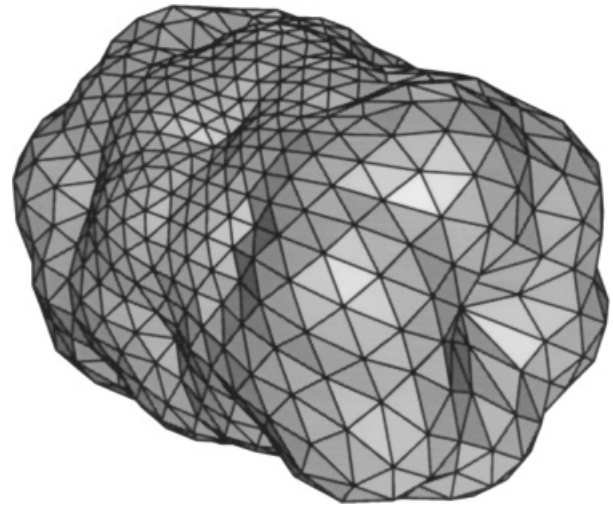

(b)

FIGURE 2. A graphical comparison of the DefPol and Gepol procedure. (a) The molecular structure of a finite-size nanotube with a molecular formula $C_{24}B_{12}N_{12}H_{12}$. (The small spheres are hydrogen atoms; the large spheres are from the darkest to the lightest nitrogen, carbon, and boron atoms.) (b) The DefPol cavity. (c) The Gepol cavity.

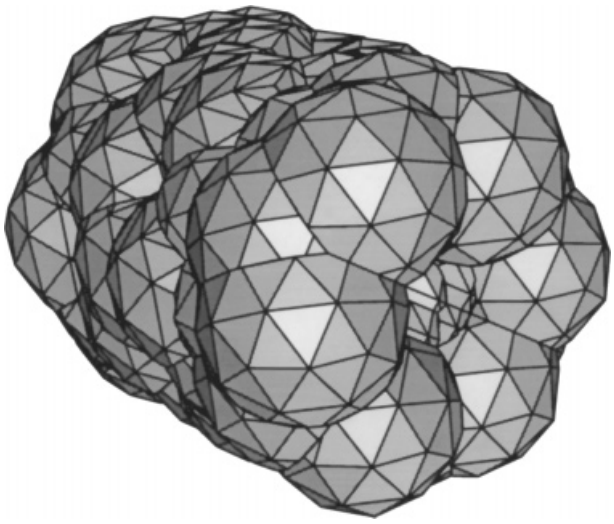

(c)

FIGURE 2. (Continued.)

of the algorithm. The occurrence of instabilities is a rare event in DefPol: we have not yet found instabilities with this new version.

A second advantage is the introduction of analytical geometry derivatives. We emphasized that an approximation was used here: similar approximations were used in other continuum solvent procedures for analytical gradients without paying much attention to the question. Actually it seems to be a good approximation for polar solvents, insofar an extreme precision is not asked, but an extreme precision on the equilibrium geometry is not realistic with the object of the study of large molecular systems.

The DefPol algorithm still presents some methodological limitations that are due to its original conception as a method for an efficient evaluation of the molecular surface for globular molecules. This excludes applications of the present DefPol version to molecules with an Euler–Poincaré characteristic different from $\chi = 2$ (homologous to the sphere). This limitation can indeed be removed by using appropriate polyhedra for other molecular topologies. We have codes, which are not inserted in Gaussian, for molecules having $\chi = 0$ and 4. Another limitation exists in the cases in which the center of mass is not a good choice for the center of projection of the vertices. An improvement can be to use more sophisticated definitions of the centers of projection, which can be different form point to point and related to local information on the molecular shape. Some enhancements to DefPol to remove these limitations are under development.

References

1. Strain, M. C.; Scuseria, G. E.; Frisch, M. J. Science 1996, 271, 51.
2. White, C. A.; Johnson, B. G.; Gill, P. M. W.; Head-Gordon, M. Chem Phys Lett 1996, 253, 268.
3. Tomasi, J.; Persico, M. Chem Rev 1994, 94, 2027.
4. Rivail, J. L.; Rinaldi, D.; Ruiz-Lopez, M. F. In Computational Chemistry: Review of Current Trends; Lecszynsky, J., Ed.; World Scientific: Singapore, 1995.
5. Cramer, C. J.; Truhlar, D. J. In Review of Computational Chemistry; Lipkowitz, K. B.; Boyd, D. B., Eds.; VCH: New York, 1995.
6. Miertus, S.; Scrocco, E.; Tomasi, J. Chem Phys 1981, 55, 117.
7. Klamt, A.; Schüürman, G. J Chem Soc Perkin Trans 1993, 2, 799.
8. Amovilli, C.; Barone, V.; Cammi, R.; Cances, E.; Cossi, M.; Mennucci, B.; Pomelli, C.; Tomasi, J. Adv Quantum Chem 1998, 32, 227.
9. Cossi, M.; Barone, V.; Cammi, R.; Tomasi, J. Chem Phys Lett 1996, 255, 327.
10. Barone, V.; Cossi, M.; Tomasi, J. J Chem Phys 1997, 107, 3210.
11. Cancés, E.; Mennucci, B.; Tomasi, J. J Chem Phys 1997, 107, 3032.
12. Cancés, E.; Mennucci, B.; Tomasi, J. J Chem Phys 1998, 109, 260.
13. Barone, V.; Cossi, M. J Phys Chem A 1998, 102, 1995.
14. Cossi, M.; Barone, V. J Chem Phys 1998, 109, 6246.
15. Rega, N.; Cossi, M.; Barone, V. Chem Phys Lett 1998, 293, 221.
16. Scalmani, G.; Barone, V. Chem Phys Lett 1999, 301, 263.
17. Rega, N.; Cossi, M.; Barone, V.; Pomelli, C. S.; Tomasi, J. Int J Quantum Chem 1999, 73, 219.
18. Pomelli, C. S.; Tomasi, J. Theor Chem Acc 1998, 99, 34.
19. Pomelli, C. S.; Tomasi, J. J Comput Chem 1998, 19, 1758.
20. Pascual-Ahuir, J. L.; Silla, E.; Tomasi, J.; Bonaccorsi, R. J Comput Chem 1987, 8, 778.
21. Frisch, M. J.; Trucks, G. W.; Schlegel, H. B.; Scuseria, G. E.; Robb, M. A.; Cheeseman, J. R.; Zakrzewski, V. G.; Montgomery, J. A.; Stratmann, R. E.; Burant, J. C.; Dapprich, S.; Millam, J. M.; Daniels, A. D.; Kudin, K. N.; Strain, M. C.; Farkas, O.; Tomasi, J.; Barone, V.; Cossi, M.; Cammi, R.; Mennucci, B.; Pomelli, C.; Adamo, C.; Clifford, S.; Ochterski, J.; Petersson, G. A.; Ayala, P. Y.; Cui, Q.; Morokuma, K.; Malick, D. K.; Rabuck, A. D.; Raghavachari, K.; Foresman, J. B.; Cioslowski, J.; Ortiz, J. V.; Stefanov, B. B.; Liu, G.; Liashenko, A.; Piskorz, P.; Komaromi, I.; Gomperts, R.; Martin, R. L.; Fox, D. J.; Keith, T.; Al-Laham, M. A.; Peng, C. Y.; Nanayakkara, A.; Gonzalez, C.; Challacombe, M.; Gill, P. M. W.; Johnson, B.; Chen, W.; Wong, M. W.; Andres, J. L.; Head-Gordon, M.; Replogle, E. S.; Pople, J. A. Gaussian 99, Development Version (Revision A.8); Gaussian, Inc.: Pittsburgh, PA, 1998.
22. Dapprich, S.; Komaroni, I.; Byun, K. S.; Morokuma, K.; Frisch, M. J. J Mol Struct (Theochem) 1999, 462, 1.
23. Herbison-Evans, D. Technical Report TR94-487; Basser Department of Computer Science, University of Sidney: Sidney, Australia.

24. Luque, F.; Bachs, M.; Aleman, C.; Orozco, M. J Comput Chem 1996, 17, 806.
25. Pierotti, R. A. Chem Rev 1976, 76, 717.
26. Claverie, P. In Intermolecular Interactions: From Diatomics to Biomolecules; Pullman, B., Ed.; Wiley: Chichester, U.K., 1978.
27. Floris, F. M.; Tomasi, J.; Pascual Ahuir, J. L. J Comput Chem 1991, 12, 784.
28. Caillet, J.; Claverie, P. Acta Crystallogr B 1978, 34, 3266.
29. Foresman, J. B.; Frisch, M. J. Exploring Chemistry with Electronic Structure Methods, 2nd ed.; Gaussian, Inc.: Pittsburgh, PA, 1996.
30. Adamo, C.; Barone, V. J Chem Phys 1999, 110, 6158.
31. Rappé, A. K.; Goddard III, W. A. J Phys Chem 1991, 95, 3358.
32. Klamt, A.; Jonas, V. J Chem Phys 1996, 150, 9972.
33. Galpern, E. G.; Pinyaskin, V. V.; Stankevich, I. V.; Chernozatonskii, L. A. J Phys Chem B 1997, 101, 705.